Modeling the Sulfate-induced Damage of Concrete

P. Dangla[1], Y. Gu[2], O. Omikrine-Metalssi[3], T. Fen-Chong[3] and R.P. Martin[4]

[1]Univ Gustave Eiffel, Ecole des Ponts, CNRS, Navier, F-77454 Marne-la-Vallée, France,
patrick.dangla@univ-eiffel.fr (P. Dangla) (Corresponding author), ,

[2]Technical research center of Finland Ltd., 02150, Espoo, Finland, yushan.gu@vtt.fi (Y. Gu), ,

[3]Univ Gustave Eiffel, CEREMA, UMR MCD, F-77454 Marne-la-Vallée, France,
othman.omikrine-metalssi@univ-eiffel.fr (O. Omikrine-Metalssi),
teddy.fenchong@univ-eiffel.fr (T. Fen-Chong), ,

[4]Univ Gustave Eiffel, MAST-EMGCU, F-77454 Marne-la-Vallée, France,
renaud-pierre.martin@univ-eiffel.fr (R.P. Martin)

Abstract. *The degradation of concrete due to sulfate attack from internal or external sources is a serious problem. The cause of this degradation is the formation and growth of ettringite, which results from the reaction of cement hydrates with sulfate ions in the pore network. This crystal growth leads to a pore pressure that can exceed the concrete's strength. This paper presents a modeling of concrete's sulfate-induced stress-strain behavior based on damage poromechanics and two kinetic laws for ettringite growth. Free expansion of cement paste samples exposed to sulfate solutions were measured, and mercury porosimetry tests were conducted at different expansion stages. The pore size distribution was analyzed to locate the dissolution of hydrates and precipitation of ettringite at the pore scale. Results support the theory that ettringite first precipitates in larger capillary pores and spreads to smaller ones. A heat-based dissolution test was performed at different expansion stages, revealing ettringite formed in the pore size range of 4-30 nm. The model was implemented in a finite volume code and applied to four experimental cases from the literature: ESA and DEF in confined and free conditions. The kinetic coefficients were calibrated to fit the observed strains in some experiments and used to blindly test the model in others. Diffusion was neglected due to the small sample size. All simulations showed that the calibrated kinetic parameters had the same order of magnitude, supporting the right physics involved.*

Keywords: *Durability; Poromechanics; Sulfate attack; Delayed ettringite formation;*

1 Introduction

Internal and external sulfate attacks are well-known phenomena of degradation of concrete. Many pieces of research have been conducted separately on these two types of attacks. However both types of degradation have the same cause: the formation of ettringite resulting from the chemical reaction between the sulfate ions and the cement hydrates. Only the source of sulfate ions and the environmental conditions differ between the two types of attack. Consequently a unique mechanism based on the crystallization pressure is expected to explain and model the two types of behavior. To provide concrete answers to this idea we conduct some experiments to analyze the location of ettringite at the pore scale and we propose a modeling based on the poromechanics and the crystallization pressure applicable to both ESA and DEF.
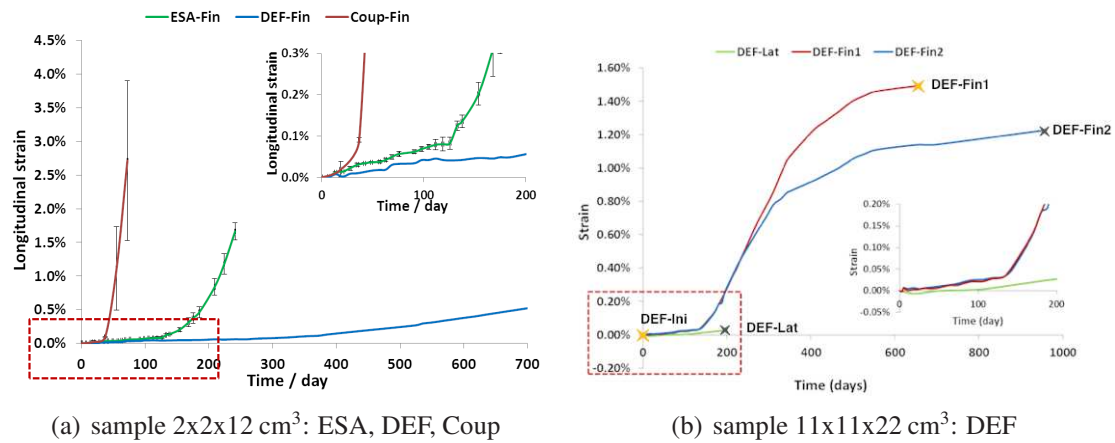
(a) sample 2x2x12 cm^3: ESA, DEF, Coup   (b) sample 11x11x22 cm^3: DEF

Figure 1. Length expansion of samples subjected to ESA, DEF and both (Coup).

2 Evolution of the pore size distribution during sulfate attack

Some experiments have been performed on cement paste samples subjected to external sulfate attack and delayed ettringite formation (Gu et al., 2019). The length expansion were monitored by equipping the samples with stainless steel pins. Typical measures of length expansion are shown in the figures (1).

In addition to that the pore size distribution of the samples were characterized by mercury porosimetry at different elapsed exposure times namely the initial state, the final degraded state where the expansion is around 1% and on some samples at the end of the latent period from which the expansion starts to accelerate. The variation of the PSD resulting from the sulfate attacks were highlighted by dividing the pores into three categories according to the variation of the pore volume after the attacks. The results are shown in the figure (2). The evolution of the pore volumes is the consequence of different processes each of them causing a decrease ($\Delta V < 0$) or an increase ($\Delta V > 0$): the crystal formation ($\Delta V < 0$), the dissolution of the portlantide ($\Delta V > 0$), the decalcification of the C-S-H ($\Delta V > 0$), the formation of micro-cracks ($\Delta V > 0$). According to some literature the pores in hardened cement paste can be divided in capillary pores (larger than 10 nm) and gel pores (less than 10 nm) (Monteiro, 2006). It is assumed that the dissolution of the portlandite causes a volume increase of capillary pores while the decalcification of C-S-H causes a volume increase of gel pores (Gerven et al., 2007; Haga et al., 2005; Saito & Deguchi, 2000). It can be concluded from the analysis of the evolution of the PSD, as illusrated in the figure (2), that ettringite forms

- in capillary and gel pores in general
- in capillary pores when expansion is limited
- first forms in the biggest pores without generating expansion
- then penetrates in capillary and gel pores from which expansion increases rapidly

These observations reinforce the idea that ettringite precipitates first in the largest pores then penetrates ever-smaller pores consistently with the Oswald-Freundlich equation.

To confirm the above analysis an innovative experiment based on the thermal stability of ettringite was conducted (Gu et al., 2020). The test is designed to empty the pores that are
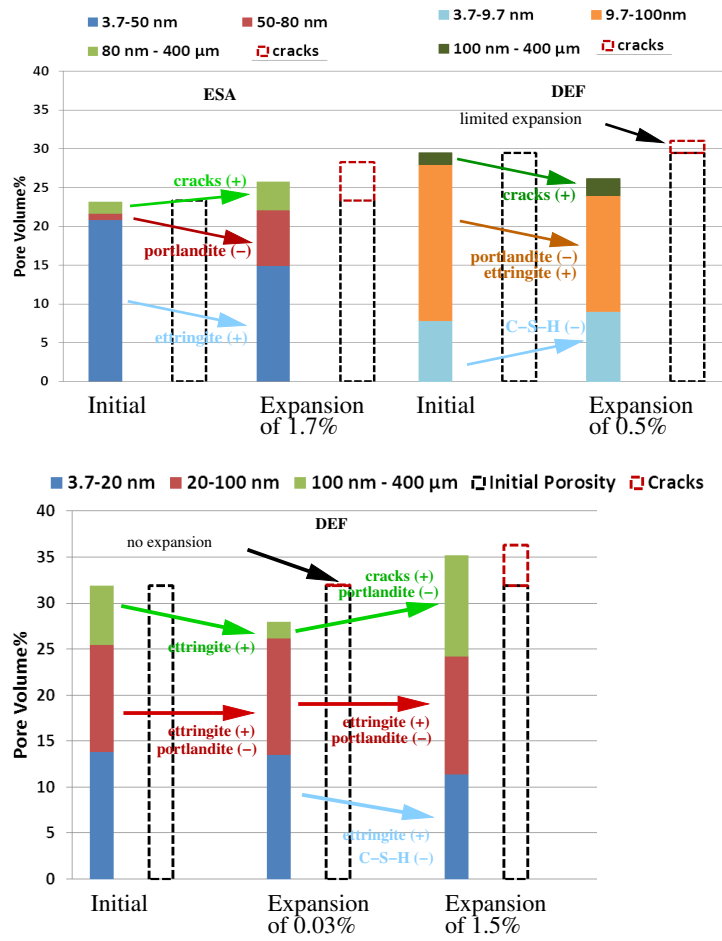
Figure 2. Pore volume variations; symbols (+)/(-) stand for gain/loss respectively.
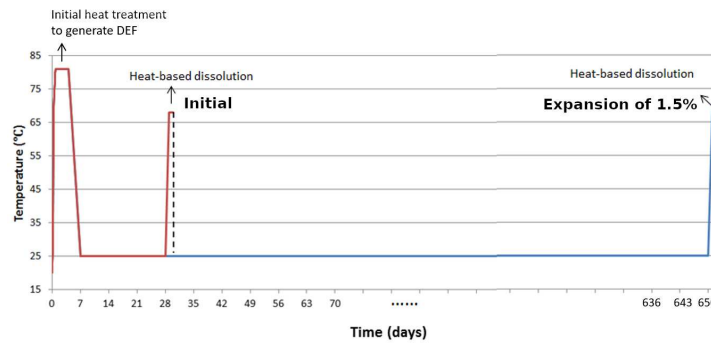
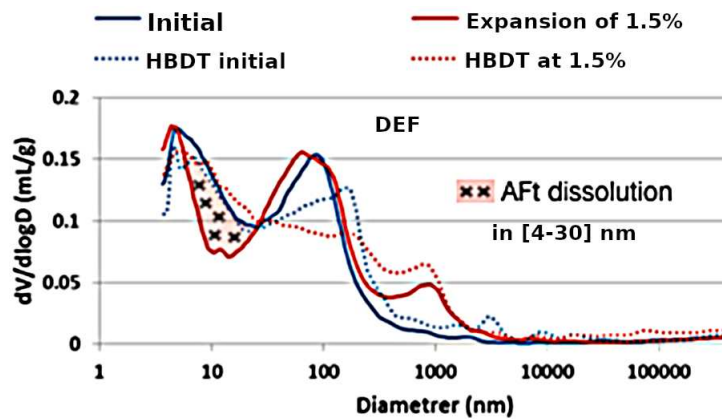**Figure 3.** Applied temperature of the heat-based dissolution test.

Figure 4. Pore size distribution of a cement paste sujected to DEF in four states: initial state, after a DEF expansion of 1.5% and in the same states after a heat-based dissolution test. In the pore range [4-30] nm the HBDT has recovered the initial pore volume which is explained by the dissolution of ettringite in this range of pore size.

filled by ettringite during their delayed formation (DEF) through a one day heating process at 68 °C called heat-based dissolution test (HBDT). Firstly the HBDT is applied to the sample in its initial state, i.e. 28 days after the DEF heat treatment with the purpose to study the effect of temperatures on the PSD of the sound samples that have no DEF-induced ettringite. Secondly the HBDT is applied to the damaged samples after an expansion of 1.5%. The PSD obtained before and after the HBDT at these two different stages are shown in the figure (4). The volume identified by the black crosses in the figure (4) corresponds to the volume of the delayed ettringite which has been released by the HBDT. This ettringite is located in the pore range 4-30 nm. The figure (4) also confirms that the HBDT leads to the formation of new portlandite in the pore range 30-100 nm.

3 Modeling

A damage poromechanical model has been adopted for the mechanical constitutive equations of the cement-based materials subjected to sulfate attack. The expansion of materials exposed to sulfate attacks is assumed to originate from the crystallization pressure exerted at the pore wall. A thin film of solution of nanometric size is acknowledged to remain between the crystal

4

and the solid wall. The growth of crystal is thus allowed by the transport of ions through the film. The stress-strain relationship is therefore given by

$$\boldsymbol{\sigma} = \mathbb{C}(d) : \boldsymbol{\epsilon} - b(d)\, S_C P_C\, \mathbf{1} \tag{1}$$

where d is the damage variable, S_C is saturation degree of the ettringite crystals and P_C is pressure exerted by the crystals on the pore wall and coined as the crystallization pressure. After the damage theory the evolution the damage variable d occurs when a criterion of the form $f(\epsilon, \kappa) = 0$ is reached. When $f(\epsilon, \kappa) < 0$ the damage does not evolve. Here we used the model proposed by Jirasek (Jirásek & Patzák, 2002).

The saturation degree of the ettringite crystals is defined as the volume fraction occupied by the crystals in the porosity. Since crystals precipitate first in the biggest pores and then penetrate ever-smaller pores consistently with the Oswald-Freundlich equation (Gu et al., 2022), the saturation degree S_C should be related to the volume of pores larger than a given size i.e. to PSD of the material. This PSD is usually derived mathematically from a function, $S(r)$, representing the volume fraction occupied by pores having a pore entry radius lower than r. This volume fraction can be characterized by mercury porosimetry or dynamic vapor sorption techniques. Therefore the saturation degree of the ettringite crystals is $S_C(r) = 1 - S(r)$. The function $S(r)$ is often fitted using the Van Genuchten model

$$S(r) = (1 + (r_0/r)^{1/(1-m)})^{-m} \tag{2}$$

To predict the expansion kinetics it is needed to model the evolution of both S_C and P_C. To this purpose we propose a crystal growth kinetics based on interface-growth mechanism.

The volume fraction of ettringite crystals in its current state, denoted with ϕ_C, is defined as the volume occupied by crystals per unit volume of material in its undeformed state. If the material were rigid, the volume $\phi_C = \phi_0 S_C$ would only result from the invasion of the porous volume. In a deformable material the volume ϕ_C should also result from the deformation of the porous volume under the action of the crystallization pressure. Accordingly the volume fraction of crystals is split into two parts:

$$\phi_C = \phi_0 S_C + \varphi_C \tag{3}$$

The second term of the right hand side, φ_C, is the volume fraction filled by crystals due only to the deformation of pores, i.e. essentially the cracks generated by the damage process. From the poromechanics it depends on the state variables: $\varphi_C(\epsilon, P_C, S_C, d)$.

The growth rate of the crystal is assumed to follow an interface-controlled mechanism as suggested by Kirkpatrick (Kirkpatrick, 1975). It follows the kinetic laws (Gu et al., 2022)

$$\frac{\mathrm{d}}{\mathrm{d}t}(\phi_0 S_C) = \phi_0 A_r (1 - \beta_r^{\mathrm{eq}}/\beta) \tag{4}$$

$$\frac{\mathrm{d}}{\mathrm{d}t}(\varphi_C) = S_C A_p (1 - \beta_p^{\mathrm{eq}}/\beta) \tag{5}$$

where A_r and A_p are two kinetic constants to be calibrated. In these equations β, β_r^{eq} and β_p^{eq}

denote saturation indices relative to the dissolved ettringite in solution: β is the current saturation index of the ettringite while β_r^{eq} and β_p^{eq}, defined by the Oswald-Freundlich and Correns equations respectively, are related to the pore radius and the crystallization pressure under the form

$$\frac{RT}{V_{\text{C}}} \ln \beta_r^{\text{eq}} = \frac{2\gamma_{\text{CL}}}{r} \tag{6}$$

$$\frac{RT}{V_{\text{C}}} \ln \beta_p^{\text{eq}} = P_{\text{C}} \tag{7}$$

The superscript 'eq' denote equilibrium. They are the saturation indices that the current solution would have taken to reach a thermodynamic equilibrium with the crystal. If the two β^{eq} are different the equilibrium is impossible. This is the case when the stress state in the crystal is anisotropic.

The computation of the stress-strain relations requires the saturation index of ettringite crystal denoted as β in the above equations. This saturation index is computed from a set of chemical equations expressing the electroneutrality of the solution and the conservation of mass for calcium and aluminium. In addition mass action law is considered for portlandite and hydrogarnet. This set of equations can be solved for β with the sulfate ion concentration $\rho_{\text{SO}_4^{2-}}$ as input (Gu et al., 2022).

4 Simulations of homogeneous cement paste exposed to sulfate attacks

We simulate the experiment performed by Ma *et al* (Ma et al., 2016). In these experiments hollow cement paste cylinders were exposed to ESA in axial restrained condition by employing a steel bar through the cylinder. The axial compression in the cement paste resulting from the ESA was measured. Two concentrations were used: 1.5 g/L and 30 g/L. The kinetic constant A_r is calibrated by using the greatest concentration and then is used as is to make prediction for the case 1.5 g/L as shown in the figure (5(a)).

We also simulate a free swelling experiment performed on mortar cylinders by Ferraris *et al* (Ferraris et al., E FN Spon, London, 1997). The specimens were exposed to sodium sulfate (49.7 g/L) with different geometries. The comparison between the experiment and the simulation in presented in figure (5(b)).

We also simulated cement paste exposed to DEF in similar conditions (Gu et al., 2022) and with different geometries. In each case the kinetic constants A_r and A_p were first calibrated with specific conditions (geometry, boundary conditions) and then used as is for prediction in other conditions.

From all these studies, it turns out that the overall range of variation of the calibrated parameters is rather limited, i.e. $[3.0 - 8.4]\ 10^{-8}\ \text{s}^{-1}$ for A_r and $[1.6 - 4.4]\ 10^{-9}\ \text{s}^{-1}$ for A_p, especially if we consider that the diffusion have been neglected in these simulations. In addition, the ratio between these coefficients turnet out to be rather constant, between 18 and 19. We believe that these rather similar factors reflect the physics of the surface-controlled growth mechanism as proposed for the kinetic laws.
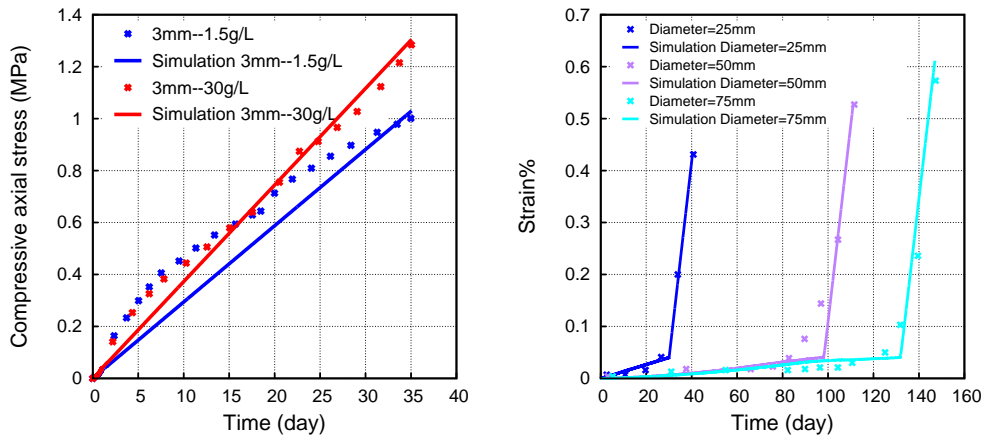
(a) Comparison of axial stress generated by ESA in a restrained hollow cement paste cylinder.

(b) Simulations of free swelling generated by ESA Ferraris et al. (E FN Spon, London, 1997)

Figure 5. Two simulations of ESA.

5 Conclusions

A poromechanical damage model based on the crystallization pressure and two kinetic laws for the growth of ettringite has been proposed. This model is intended to address both ESA and DEF except for their different source of sulfates. This model relies on two kinetic parameters. It is applied to cement paste exposed to sulfate attack in different conditions and compare with experiments. It can describe rather satisfactorily the swelling and the stresses induced by the attack. The following major conclusions are

- Surface-controlled growth mechanism is relevant for both ESA and DEF.
- Whether it is for ESA or DEF, the deformation originate from the same mechanisms except from what concerns the source of sulfate ions.
- The latent period during which minimal deformation occurs is an elastic response of the material where ettringite crystals first fill the biggest pores and generate small crystallization pressure and tensile effective stresses.
- The accelerated period starts when the amount of crystal and the crystallization pressure are such that the effective stress - strain relationship results from the damage process and the post-peak tensile behavior of the material.
- When the pH is low gypsum should be considered for a possible source of crystallization pressure instead of ettringite.

References

Ferraris, C., Clifton, J., Stutzman, P., & Garboczi, E. (E FN Spon, London, 1997). Mechanics of degradation of portland cement-based systems by sulfate attack. *Ch. 22 in Mechanisms of Chemical Degradation of Cement-based Systems, eds..* (K.L. Scrivener and J.F. Young. ISBN: 0419215700)

Gerven, T. V., Cornelis, G., Vandoren, E., & Vandecasteele, C. (2007). Effects of carbonation and leaching on porosity in cement-bound waste. *Waste Manag.*, *27*(7), 977–985.

Gu, Y., Dangla, P., Martin, R.-P., Omikrine Metalssi, O., & Fen-Chong, T. (2022). Modeling the sulfate attack induced expansion of cementitious materials based on interface-controlled

crystal growth mechanisms. *Cement and Concrete Research*, *152*, 106676. Retrieved from https://www.sciencedirect.com/science/article/pii/S0008884621003252 doi: https://doi.org/10.1016/j.cemconres.2021.106676

Gu, Y., Martin, R.-P., Metalssi, O. O., Fen-Chong, T., & Dangla, P. (2019). Pore size analyses of cement paste exposed to external sulfate attack and delayed ettringite formation. *Cement and Concrete Research*, *123*, 105766. doi: https://doi.org/10.1016/j.cemconres.2019.05.011

Gu, Y., Omikrine Metalssi, O., Martin, R.-P., Fen-Chong, T., & Dangla, P. (2020). Locating ettringite due to def at the pore scale of cement paste by heat-based dissolution tests. *Construction and Building Materials*, *258*, 120000. Retrieved from http://www.sciencedirect.com/science/article/pii/S0950061820320055 doi: https://doi.org/10.1016/j.conbuildmat.2020.120000

Haga, K., Sutou, S., Hironaga, M., Tanaka, S., & Nagasaki, S. (2005). Effects of porosity on leaching of ca from hardened ordinary portland cement paste. *Cem. Concr. Res.*, *35*(9), 1764–1775.

Jirásek, M., & Patzák, B. (2002). Consistent tangent stiffness for nonlocal damage models. *Computers & Structures*, *80*(14-15), 1279–1293. (https://doi.org/10.1016/S0045-7949(02)00078-0)

Kirkpatrick, R. J. (1975). Crystal growth from the melt: A review. *American Mineralogist: Journal of Earth and Planetary Materials*, *60*(9-10), 798–814.

Ma, X., Çopuroğlu, O., Schlangen, E., Han, N., & Xing, F. (2016). Experimental and numerical study on cement paste degradation under external sulfate attack. In *Proceedings of 9th international conference on fracture mechanics of concrete and concrete structures.* (https://doi.org/10.21012/FC9.088)

Monteiro, P. (2006). *Concrete: microstructure, properties, and materials*.

Ran, B., Li, K., Fen-Chong, T., Omikrine-Metalssi, O., & Dangla, P. (2022). Spalling rate of concretes subject to combined leaching and external sulfate attack. *Cement and Concrete Research*, *162*, 106951. Retrieved from https://www.sciencedirect.com/science/article/pii/S0008884622002435 doi: https://doi.org/10.1016/j.cemconres.2022.106951

Ran, B., Omikrine-Metalssi, O., Fen-Chong, T., Dangla, P., & Li, K. (2023). Pore crystallization and expansion of cement pastes in sulfate solutions with and without chlorides. *Cement and Concrete Research*, *166*, 107099. Retrieved from https://www.sciencedirect.com/science/article/pii/S000888462300011X doi: https://doi.org/10.1016/j.cemconres.2023.107099

Saito, H., & Deguchi, A. (2000). Leaching tests on different mortars using accelerated electrochemical method. *Cem. Concr. Res.*, *30*(11), 1815–1825.